Supplemental Materials

Quantum spin–quantum anomalous Hall effect with tunable edge states in Sb monolayer-based heterostructures

Tong Zhou[1], Jiayong Zhang[1], Yang Xue[1], Bao Zhao[1], Huisheng Zhang[1], Hua Jiang[2,], and Zhongqin Yang[1,3,*]*

1 State Key Laboratory of Surface Physics and Key Laboratory for Computational Physical Sciences (MOE) & Department of Physics, Fudan University, Shanghai 200433, China

2 College of Physics, Optoelectronics and Energy, Soochow University, Suzhou (215006), China

3 Collaborative Innovation Center of Advanced Microstructures, Fudan University, Shanghai 200433, China

The opening mechanisms of the QAH/QSH gaps

The QAH/QSH gaps are determined by the competition between M_A (M_B) and λ_{SO}, deduced as follows. For the basis,

$$\Phi_i = \{|\phi^A_{+,\uparrow}>, |\phi^A_{+,\downarrow}>, |\phi^A_{-,\uparrow}>, |\phi^A_{-,\downarrow}>, |\phi^B_{+,\uparrow}>, |\phi^B_{+,\downarrow}>, |\phi^B_{-,\uparrow}>, |\phi^B_{-,\downarrow}>\},$$

$$|\phi^{A/B}_{+,\uparrow}> = -\frac{1}{\sqrt{2}}(p^{A/B}_{x,\uparrow} + ip^{A/B}_{y,\uparrow}), \quad |\phi^{A/B}_{+,\downarrow}> = -\frac{1}{\sqrt{2}}(p^{A/B}_{x,\downarrow} + ip^{A/B}_{y,\downarrow}),$$

$$|\phi^{A/B}_{-,\uparrow}> = \frac{1}{\sqrt{2}}(p^{A/B}_{x,\uparrow} - ip^{A/B}_{y,\uparrow}), \quad |\phi^{A/B}_{-,\downarrow}> = \frac{1}{\sqrt{2}}(p^{A/B}_{x,\downarrow} - ip^{A/B}_{y,\downarrow}).$$

The Hamiltonian of Eq. (3) in k-space is given by an 8×8 matrix as

$$H = H_U + H_{SO} + H_M + H_T + H_R \quad ,$$

where H_U, H_{SO}, H_M, H_T, and H_R express the staggered potential for the A(B) sublattice, intrinsic SOC, magnetic exchange field, nearest-neighboring hopping term, and extrinsic Rashba SOC, respectively. Concretely,

$$H_U = \begin{bmatrix} U & 0 & 0 & 0 & 0 & 0 & 0 & 0 \\ 0 & U & 0 & 0 & 0 & 0 & 0 & 0 \\ 0 & 0 & U & 0 & 0 & 0 & 0 & 0 \\ 0 & 0 & 0 & U & 0 & 0 & 0 & 0 \\ 0 & 0 & 0 & 0 & -U & 0 & 0 & 0 \\ 0 & 0 & 0 & 0 & 0 & -U & 0 & 0 \\ 0 & 0 & 0 & 0 & 0 & 0 & -U & 0 \\ 0 & 0 & 0 & 0 & 0 & 0 & 0 & -U \end{bmatrix};$$

$$H_{SO}=\begin{bmatrix} \lambda so & 0 & 0 & 0 & 0 & 0 & 0 & 0 \\ 0 & -\lambda so & 0 & 0 & 0 & 0 & 0 & 0 \\ 0 & 0 & -\lambda so & 0 & 0 & 0 & 0 & 0 \\ 0 & 0 & 0 & \lambda so & 0 & 0 & 0 & 0 \\ 0 & 0 & 0 & 0 & \lambda so & 0 & 0 & 0 \\ 0 & 0 & 0 & 0 & 0 & -\lambda so & 0 & 0 \\ 0 & 0 & 0 & 0 & 0 & 0 & -\lambda so & 0 \\ 0 & 0 & 0 & 0 & 0 & 0 & 0 & \lambda so \end{bmatrix};$$

$$H_{M}=\begin{bmatrix} M_A & 0 & 0 & 0 & 0 & 0 & 0 & 0 \\ 0 & -M_A & 0 & 0 & 0 & 0 & 0 & 0 \\ 0 & 0 & M_A & 0 & 0 & 0 & 0 & 0 \\ 0 & 0 & 0 & -M_A & 0 & 0 & 0 & 0 \\ 0 & 0 & 0 & 0 & M_B & 0 & 0 & 0 \\ 0 & 0 & 0 & 0 & 0 & -M_B & 0 & 0 \\ 0 & 0 & 0 & 0 & 0 & 0 & M_B & 0 \\ 0 & 0 & 0 & 0 & 0 & 0 & 0 & -M_B \end{bmatrix};$$

$$H_T = T_{\delta_1} e^{ik_x a} + T_{\delta_2} e^{-i(k_x a/2 - k_y\sqrt{3}a/2)} + T_{\delta_3} e^{-i(k_x a/2 + k_y\sqrt{3}a/2)},$$

where $T_{\delta_1}=\begin{bmatrix} t_1 & t_2 \\ t_2 & t_1 \end{bmatrix}\otimes\sigma_0$, $T_{\delta_2}=\begin{bmatrix} t_1 & z^2 t_2 \\ z t_2 & t_1 \end{bmatrix}\otimes\sigma_0$, $T_{\delta_3}=\begin{bmatrix} t_1 & z t_2 \\ z^2 t_2 & t_1 \end{bmatrix}\otimes\sigma_0$;

$$H_R = T_{R\delta_1} e^{ik_x a} + T_{R\delta_2} e^{-i(k_x a/2 - k_y\sqrt{3}a/2)} + T_{R\delta_3} e^{-i(k_x a/2 + k_y\sqrt{3}a/2)}, \text{ where}$$

$T_{R\delta_1}=-i\begin{bmatrix} \lambda_R & \lambda_R^{'} \\ \lambda_R^{'} & \lambda_R \end{bmatrix}\otimes\sigma_y$, $T_{R\delta_2}=i\begin{bmatrix} \lambda_R & z^2\lambda_R^{'} \\ z\lambda_R^{'} & \lambda_R \end{bmatrix}\otimes(\frac{\sqrt{3}}{2}\sigma_x+\frac{1}{2}\sigma_y)$, $T_{R\delta_3}=i\begin{bmatrix} \lambda_R & z\lambda_R^{'} \\ z^2\lambda_R^{'} & \lambda_R \end{bmatrix}\otimes(-\frac{\sqrt{3}}{2}\sigma_x+\frac{1}{2}\sigma_y)$.

Since the extrinsic Rashba term is usually smaller than the M_A (M_B) and λ_{SO} terms, we tentatively set $\lambda_R=\lambda_R^{'}=0$ to explore the competitive relationship between the M_A (M_B) and λ_{SO} terms. At the K point with $k_x=0,\ k_y=\frac{4\pi}{3\sqrt{3}a}$, where a is the lattice parameter of unit cell, the Hamiltonian

$$H_K=\begin{bmatrix} U+M_A+\lambda so & 0 & 0 & 0 & 0 & 0 & 3t_2 & 0 \\ 0 & U-M_A-\lambda so & 0 & 0 & 0 & 0 & 0 & 3t_2 \\ 0 & 0 & U+M_A-\lambda so & 0 & 0 & 0 & 0 & 0 \\ 0 & 0 & 0 & U-M_A+\lambda so & 0 & 0 & 0 & 0 \\ 0 & 0 & 0 & 0 & -U+M_B+\lambda so & 0 & 0 & 0 \\ 0 & 0 & 0 & 0 & 0 & -U-M_B-\lambda so & 0 & 0 \\ 3t_2 & 0 & 0 & 0 & 0 & 0 & -U+M_B-\lambda so & 0 \\ 0 & 3t_2 & 0 & 0 & 0 & 0 & 0 & -U-M_B+\lambda so \end{bmatrix}.$$

The energy levels at this K point can be obtained by diagonalizing above matrix. Around the E_F, the energy levels can be analytically expressed as $E_1 = \lambda so + M_B - U$, $E_2 = \lambda so - M_A + U$, $E_3 = -\lambda so + M_A + U$, and $E_4 = -\lambda so - M_B - U$. Hence, when $E_2 > E_3$, i.e. $\lambda_{SO} > M_A$, there is a QSH gap at the K point. When $E_2 < E_3$, i.e. $\lambda_{SO} < M_A$, the energy levels are inverted at the K point and a QAH gap will be achieved at the K point after the Rashba interaction is considered. Similarly, at the K' point with $k_x = 0,\ k_y = \dfrac{8\pi}{3\sqrt{3}a}$,

$$H_{K'}=\begin{bmatrix} U+M_A+\lambda so & 0 & 0 & 0 & 0 & 0 & 0 & 0 \\ 0 & U-M_A-\lambda so & 0 & 0 & 0 & 0 & 0 & 0 \\ 0 & 0 & U+M_A-\lambda so & 0 & 3t_2 & 0 & 0 & 0 \\ 0 & 0 & 0 & U-M_A+\lambda so & 0 & 3t_2 & 0 & 0 \\ 0 & 0 & 3t_2 & 0 & -U+M_B+\lambda so & 0 & 0 & 0 \\ 0 & 0 & 0 & 3t_2 & 0 & -U-M_B-\lambda so & 0 & 0 \\ 0 & 0 & 0 & 0 & 0 & 0 & -U+M_B-\lambda so & 0 \\ 0 & 0 & 0 & 0 & 0 & 0 & 0 & -U-M_B+\lambda so \end{bmatrix}.$$

The energy levels near the E_F are $E_1' = \lambda so + M_A + U$, $E_2' = \lambda so - M_B - U$, $E_3' = -\lambda so + M_B - U$, $E_4' = -\lambda so - M_A + U$. When $\lambda so > M_B$, there is a QSH gap at the K' point. When $\lambda so < M_B$, the energy levels are inverted at the K' point and a QAH gap can be achieved at the K' point after the Rashba interaction is considered. Thus, the competition of the M_A (M_B) and λ_{SO} terms can result in various topological transitions. When $\lambda_{SO} = M_A$ (M_B), it gives the phase boundaries of the topological transitions.

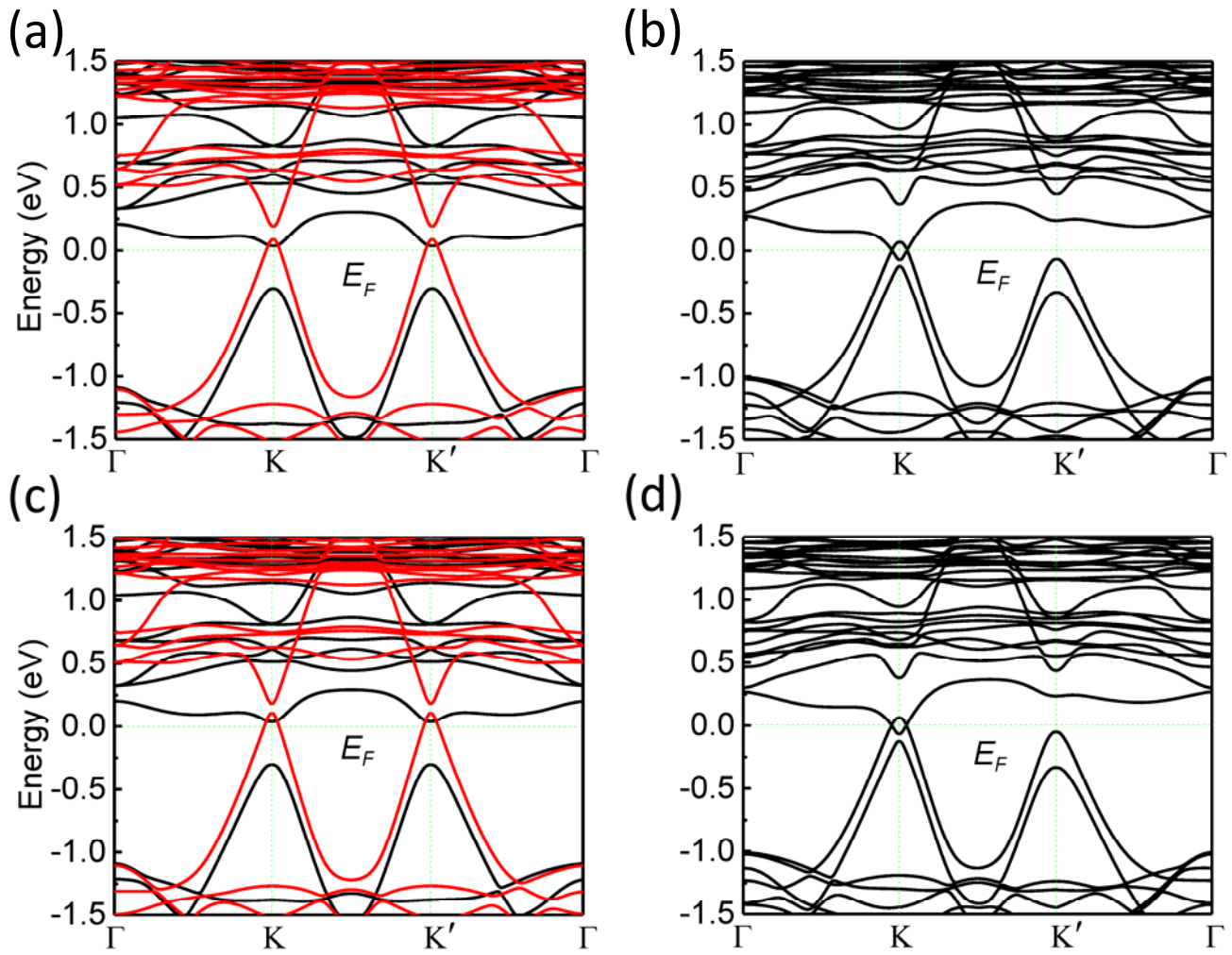

Fig. S1. (a) and (b) Band structures for the $Sb_2Cl/LaFeO_3$ heterostructure without and with SOC considered, respectively. The red and black curves denote the spin-up and spin-down states, respectively. (c) and (d) are the same as (a) and (b) except for $Sb_2Br/LaFeO_3$ heterostructure instead.

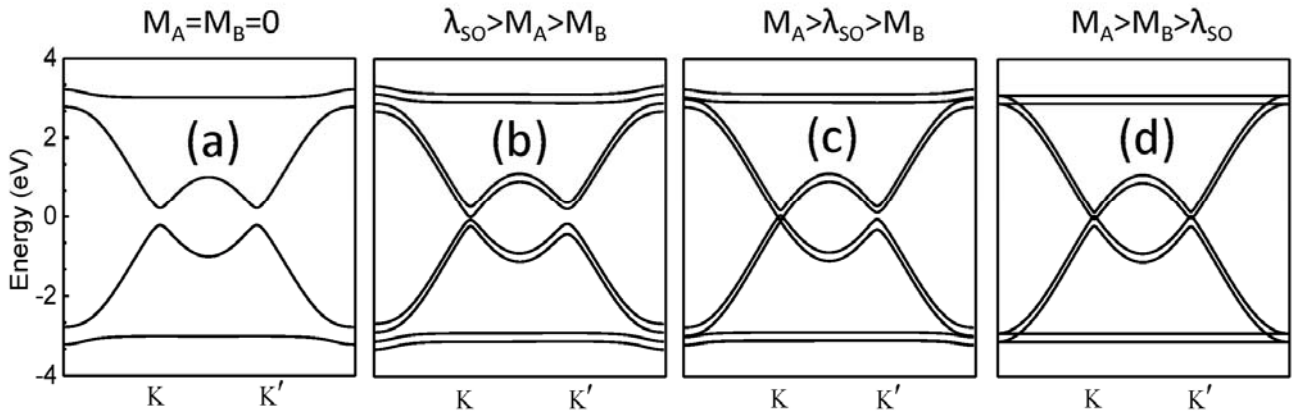

Fig. S2. (a)-(d) Band structure in large energy scale calculated from the TB model with the same TB parameters as in Fig. 4a-d, respectively.

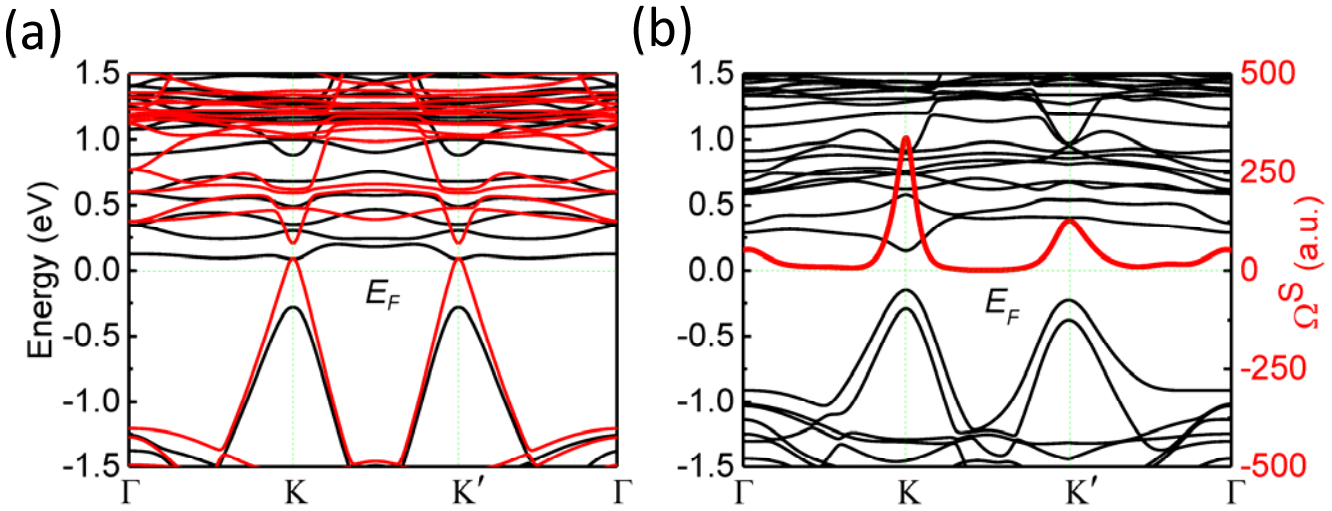

Fig. S3. (a) and (b) Band structures for the heterostructure of a hydrogenated Bi monolayer on the $LaFeO_3$ (111) surface without and with SOC considered, respectively. The red and black curves in (a) denote the spin-up and spin-down states, respectively. The red dots in (b) denote the spin Berry curvatures (in atomic units (a.u.)) for the whole valence bands.

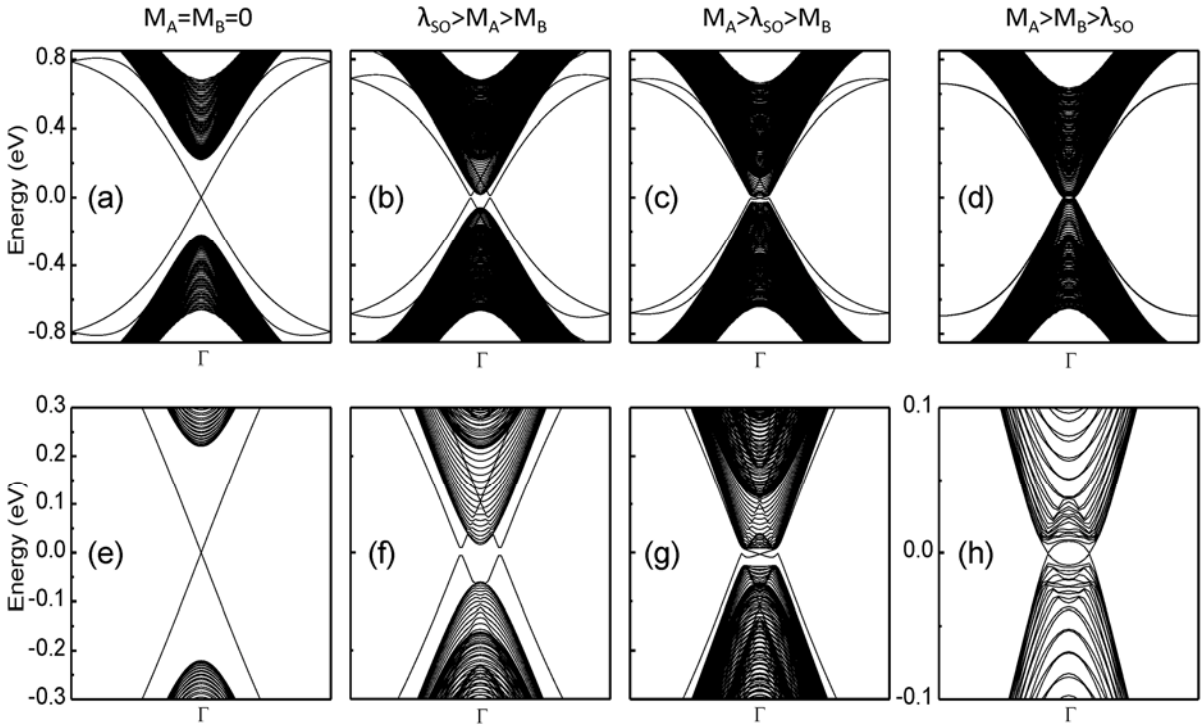

Fig. S4. (a)-(d) The band structures of the armchair nanoribbon (containing 320 atoms in the width) with the same TB parameters as Fig. 4e-h, respectively. (e)-(h) The magnified bands of (a)-(d), respectively.